Talanta 226 (2021) 122089

Contents lists available at ScienceDirect

Talanta

journal homepage: www.elsevier.com/locate/talanta

A straightforward and reliable evaluation of Ag(I) binding affinity mediated by a peptide ligand for constructing an efficient sensing platform

Xin-Yi Li, Xiao-Dong Zhou *, Ji-Ming Hu **

The Centre of Analysis and Measurement of Wuhan University, Wuhan University, Wuhan, 430072, PR China

ARTICLE INFO

Keywords:
Ag(I) affinity
Peptide-mediated calculation
Ligands selection
Biosensor design
Ag(I) detection

ABSTRACT

The reliable determination of the Ag(I) affinity for biomolecules is an essential issue in the fields of structural analysis and sensor design. However, the urgent problem confronting researchers is lack of a direct and accurate Ag(I) affinity evaluation as a reference standard for ligand analysis. We communicated here a straightforward and high-efficiency method of measuring Ag(I) affinity exactly on the basis of the unique calculation algorithm and the design of a special peptide RFPRDD (P) as Ag(I) binding motif. According to UV–vis competition between the corresponding complexes (AgP) and biomolecules (peptides, amino acids and ssDNA), the decrease of the signature at 300 nm characteristic of AgP was obtained for quantitative analysis. The primary advantages of this strategy were the widespread application, high accuracy and reference significance, which were corroborated by theoretical calculations. To identify its potential in biosensing, two kinds of testing models for Ag(I) were proposed by AgBP2-decorated and Ag4-decorated gold nanoparticles, the detection limits of which were 2 nM and 75 nM respectively. By contrast of the sensing property of the functional peptides (AgBP2, Ag4), we afforded evidence that this conception could be regarded as an evaluation criterion for the selection and performance optimization of sensitive elements, thereby holding a dominant position in the biosensors.

1. Introduction

The coordination interaction between Ag(I) and biomolecules play key biological roles in different fields, including biosensors, cell toxicity, chemical treatment and antibacterial materials [1–10]. Such biomolecules include amino acids, ssDNA and peptides, especially the well-known Ag-binding peptides (e.g. AgBP2, Ag4, AgP35) greatly involved in biosensing or silver material synthesis [11–20]. Despite the fact that numerous applications have been made possible [21–23], its future perspectives in broader application still face challenges from lacking identification and comparison of Ag(I) affinity to biomolecules.

Determining the affinity of Ag(I) is urgently needed in the field of sensing technology, first because this is intrinsically a basic parameter that mirrors the possibility to have the metal ion-biomolecules interaction under biological conditions, and second because it give insights into the coordination ability of biomolecules to Ag(I), assisting in estimating the interference of complex systems and selecting the optimum ligands for targets identification [24]. This information is absolutely vital not only for seeking out the fitter molecules (i.e., estimating for which molecules the method will be effective) but also for the design and potential of any sensor. Yet, this is an intricate task, since the affinity assessment of metal ions is always plagued by the tedious and ineffective process of analysis and numerical calculation [25–27].

For the sake of resolving this matter, much more efforts are concentrated on creating a new pathway to simplify the evaluation procedure. To this end, there are mainly two means of appraising affinity values [24]. The first one relies on potentiometric titrations that could be extremely tough to implement in the case of biomolecules and necessitate an important quantity of the biological material [25,28]. The second one mainly consists in measurements by competition experiments with a ligand of known affinity followed by the truly fitting way. In the comprehensive consideration, competition experiments appear to be well-suited to offer a practical research platform for coordination interaction and affinity calculation. On account of few studies on the Ag (I) affinity, several reports aiming at copper ions affinity are available as a methodological reference. In a pioneering work, four peptides labelled with fluorescent dyes were designed [27]. And the Cu(II) affinities for different peptides and proteins were probed by competition monitored

* Corresponding author.
** Corresponding author.
E-mail addresses: zhouxd@whu.edu.cn (X.-D. Zhou), jmhu@whu.edu.cn (J.-M. Hu).

https://doi.org/10.1016/j.talanta.2021.122089
Received 8 October 2020; Received in revised form 29 December 2020; Accepted 3 January 2021
Available online 11 January 2021

Scheme 1. Schematic drawing of the competition experiment.

by fluorescence. While Cu(II) quenched the fluorescence of the specific ligands, the addition of the targets restored it by removing the Cu(II) from the probes. In spite of good reliability, this program suffered from poor operation and complicated calculation. To combat the situation, a new dye L was synthesized for the study of Cu(II) affinity by UV–vis competition experiments [24]. And the affinity valuation could be realized by capturing the changes in characteristic signals of the CuL complexes during the competition. On this basis, more than 17 peptides derived from the human Aβ peptide were investigated. Obviously, it held overwhelming superiority in practical applications because of the simplicity and convenience. Enlighten by these evaluation systems, the objective of this protocol is to define a universal tool for rapid, straightforward and accurate determination of the Ag(I) affinity.

Herein, a novel peptide RFPRDD was engineered as the Ag(I) ligand with moderate affinity ($8.19 \pm 0.4 \times 10^7$ M^{-1} at pH 7.4). After their complexation, a UV–vis characteristic peak at 300 nm would appear, which was perfectly appropriate for quantification of Ag(I) affinity. The competition could be constituted by addition of targets in the colored Ag(I)-RFPRDD complex solution, thereby leading to the disappearance of the absorption band (Scheme 1). Using the peptide ligand, an expedient and high-efficiency calculation for Ag(I) affinity was established. Aside from directly comparing relative Ag-binding peptides in the Ag(I) affinity ability, we also made a thorough inquiry about a series of artificial peptides and ssDNA. Moreover, the prominent reliability and validity of

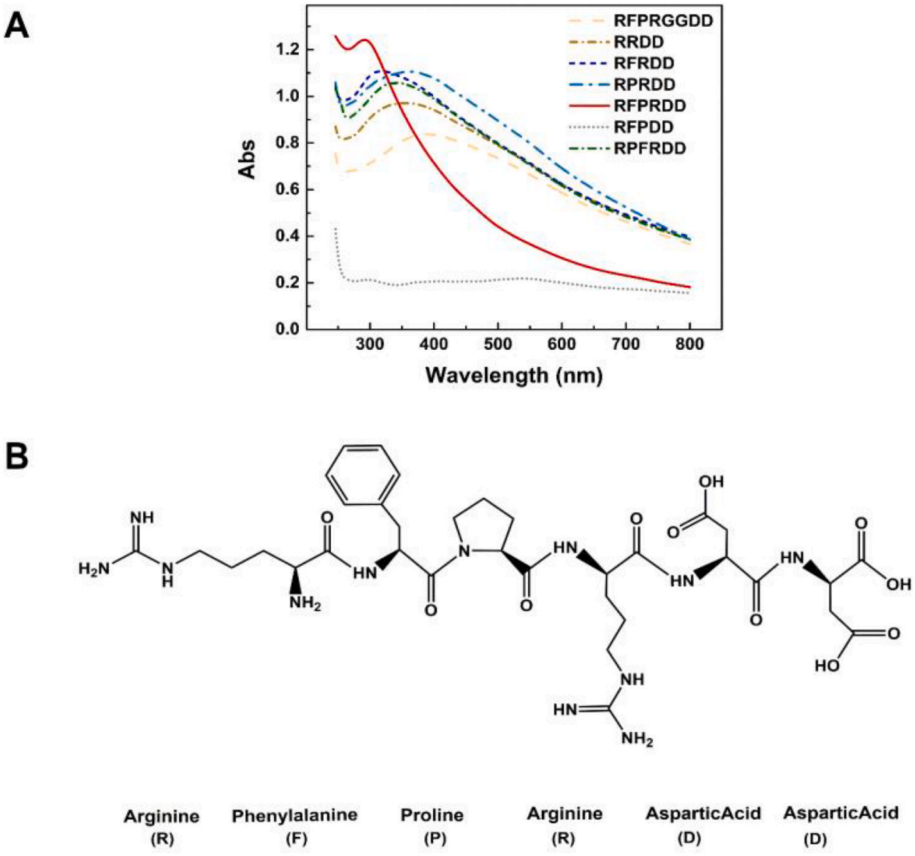

Fig. 1. (A) UV–vis spectra of different peptides (80 μM) treated with 0.9 equivalent of Ag(I). (B) Chemical structure illustrations of the peptide RFPRDD.

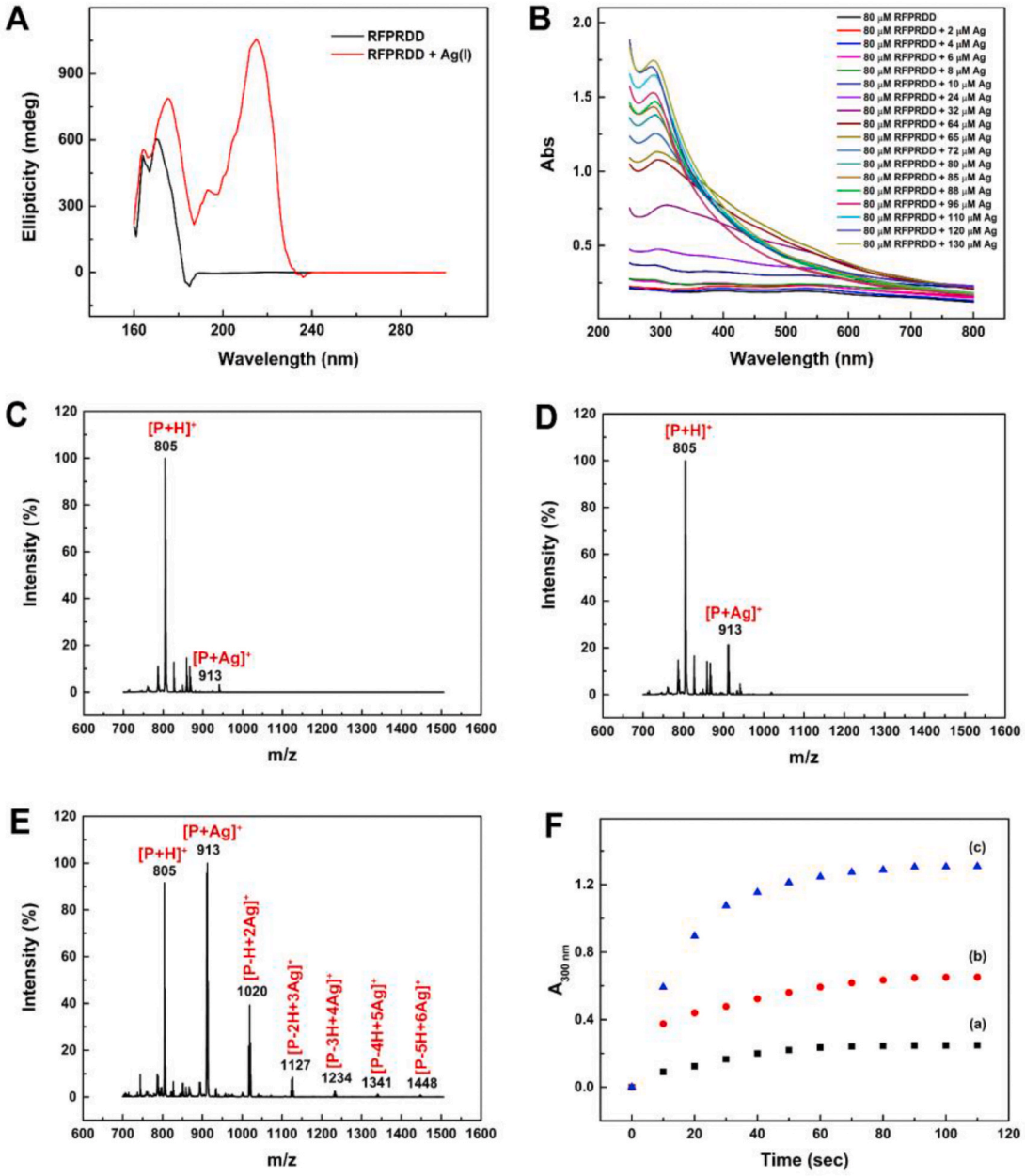

Fig. 2. (A) CD spectral analysis of Ag(I)-RFPRDD coordination. (B) UV–vis spectra of the peptide RFPRDD (80 μM) treated with different concentrations of Ag(I). MALDI-TOF Mass spectra of the peptide RFPRDD treated with (C) a small quantity of Ag(I), (D) a moderate quantity of Ag(I) or (E) a large quantity of Ag(I). (F) The absorbance at 300 nm of the mixture solution as a function of incubation time. The mixture solution contained 10 mM PB, 80 μM RFPRDD, and different concentrations of Ag(I): (a) 8 μM (b) 28 μM (c) 72 μM.

this strategy were affirmed by examining multiple amino acids with Ag (I) affinities known. Through two detection systems relying on AgBP2-capped and Ag4-capped gold nanoparticles (AuNPs), we proved that the evaluation approach could offer beneficial reference for the optimization of biosensing units, favoring the construction of detecting sensors.

2. Material and methods

2.1. Chemicals and materials

Peptides listed in Table S1 and ssDNA listed in Table S2 were obtained from Sangon Biotechnology Inc. (Shanghai, China). Ethylenediaminetetraacetic acid (EDTA), $AgNO_3$ were purchased from Sinopharm Chemical Reagent (China). Phosphate buffer (PB) was freshly prepared as the buffer solution. All the solutions and buffers in the experiments were prepared using sterile water.

2.2. Instrumentations

A Shimadzu UV-2550 was employed to obtain the absorption spectra of peptide before and after the addition of Ag(I). Mass spectra were obtained using a MALDI-TOF MS (AB SCIEX TOF/TOF 5800) instrument, using detection by reflection to generate the spectra. And CD spectra of the Ag(I)-RFPRDD complexes was collected on a Jasco J-815 CD spectrometer using a quartz cuvette with a 0.5 cm pathlength.

2.3. Synthesis of the Ag(I)-RFPRDD complexes

Briefly, the peptides RFPRDD were dissolved in PB (10 mM, pH 7.4).

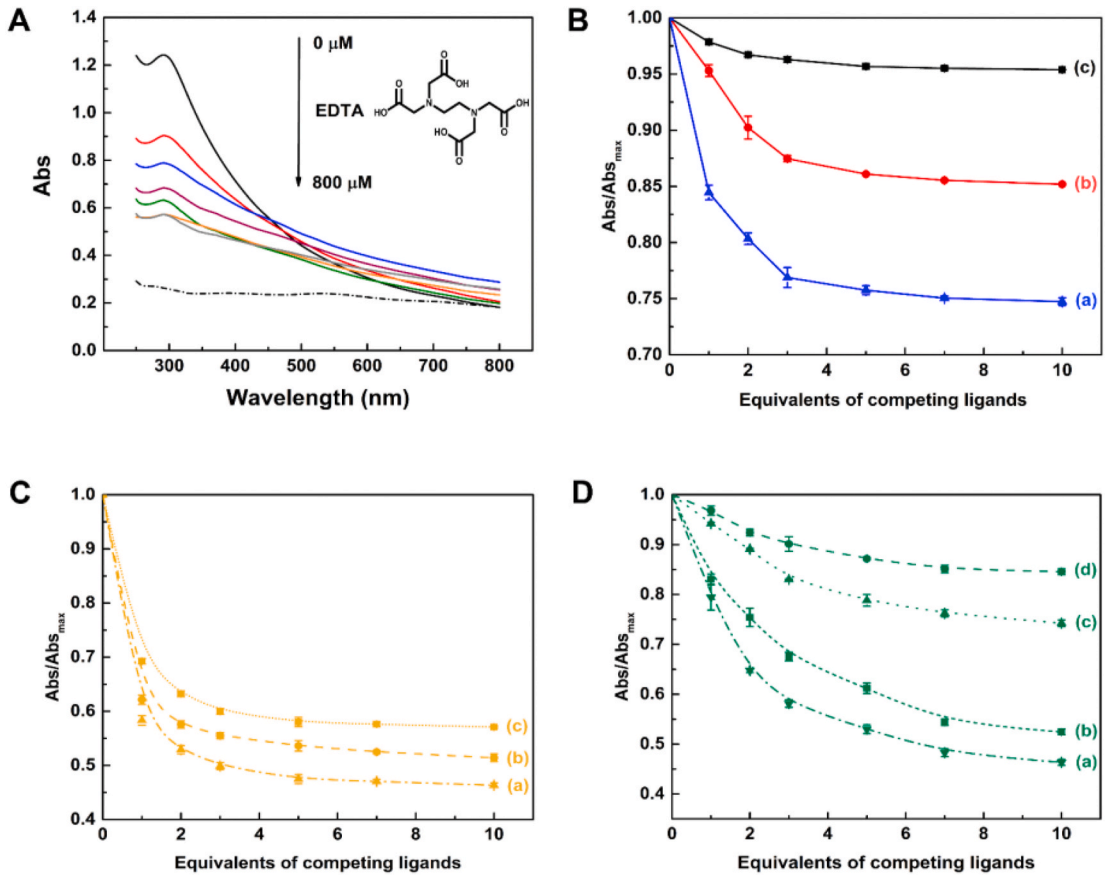

Fig. 3. (A) UV–vis spectra of the AgP complexes treated with different concentrations of EDTA. The dotted line comes from the blank RFPRDD. (B) Experimental absorbance (points) and the best fits (solid lines) of the AgP system upon addition of the competing ligands (Targets): (a) Tryptophan, (b) Histidine, (c) Methionine. Experimental absorbance (points) and the best fits (dotted lines) of the AgP system upon addition of the competing ligands (Targets): (C): (a) AgBP2, (b) Ag4, (c) AgP35; (D): (a) NAPC, (b) AgNSB, (c) NAP, (d) IH6. [P] = 80 μM, [Ag(I)] = 72 μM, [Target] = 0–800 μM, pH = 7.4, T = 25 °C (where mentioned).

Then, 80 μM peptides were added to $AgNO_3$ solution. The reaction mixture was incubated at room temperature (25 °C) for 80 s. Finally, the Ag(I)-RFPRDD complexes were obtained.

2.4. Synthesis of AuNPs and peptide-capped AuNPs

According to previously published methods, AuNPs of different sizes were obtained by the reduction of the $HAuCl_4$ salt [33]. Typically, 50 mL of 0.01% (w/w) $HAuCl_4$ was heated by boiling under vigorous magnetic stirring, followed by the addition of 11.4 mg/mL sodium citrate solution. The mixture was continuously boiled and magnetically stirred for 20 min until it turned red, and then cooled to room temperature. Finally, AuNPs were obtained and stored at 4 °C.

Briefly, the peptides (CALNN-AgBP2 or CALNN-Ag4) were dissolved in PB (10 mM, pH 7.4). Then, 50 μM peptides were added to AuNPs solution. The reaction mixture was incubated at room temperature for overnight. The free peptides were isolated by centrifugation at 6000 rpm for 15 min and finally, the peptide-modified AuNPs were prepared.

2.5. Competition experiments between the ligand and the target

The experiments have been monitored by UV–vis in 10 mM PB buffer (at a resulting pH = 7.4). The peptide ligand (80 μM) and Ag(I) (72 μM) were mixed, followed by adding different targets (0–800 μM in total). Each addition of the target is made once the thermodynamic equilibrium of the previous reaction is reached (this takes about 80 s). To be reproducible with respect to pH condition, the same stock buffer solution (pH 7.4) was employed for all the experiments. The competition experiments were executed at room temperature (25 °C).

2.6. Analysis of the data

The data analysis was performed with the following procedure for each experiment.

The absorbance of the competition experiments measured at 300 nm after completion of the reaction was plotted as a function of the number of peptides equivalents. Absorbance was calculated according to

$$\mathrm{Abs} = \varepsilon^{P}\,[P] + \varepsilon^{AgP}\,[AgP] + \varepsilon^{T}\,[T] + \varepsilon^{AgTn}\,[AgT_n]$$

Where P stands for the peptide RFPRDD, T for the target, and AgP and AgT_n for the complex between Ag(I) and peptide and the target, respectively. And n represents the coordination number of the target to Ag(I).

The same equation can be expressed as

$$\mathrm{Abs} = \varepsilon^{P}\,([P]_0\text{-}[Ag]_0\text{+}[\alpha]) + \varepsilon^{AgP}\,([Ag]_0\text{-}[\alpha]) + \varepsilon^{T}\,([T]_0\text{-}n\,[\alpha]) + \varepsilon^{AgTn}\,[\alpha]$$

Where α stands for the progression of the following reaction: peptide + Ag(I) → peptide-Ag(I) and the $[\ ]_0$ correspond to the starting values in which the dilution due to addition of the peptide has been taken into account when required.

Ag(I) is supposed to be chelated by the RFPRDD or by targets;

$$K_a^{AgT_n} \Big/ K_a^{AgP} = \frac{[AgT_n]}{[Ag]\cdot[T]^n} \cdot \frac{[Ag]\cdot[P]}{[AgP]}$$

with the starting concentrations:

Table 1
Ag(I) affinity values of the biomolecules studied here.

Biomolecules	Ref.	The coordination mode (Target: Ag(I))	K_a
AgBP2	Sedlak et al., 2012	1:1	6.30 ±0.5 × 10^7
Ag4	Naik et al., 2004; Jo et al., 2014	1:1	4.83 ±0.2 × 10^7
AgP35	Naik et al., 2004; Jo et al., 2014	1:1	2.48 ±0.7 × 10^7
NAPC	Lupaescu et al., 2019	1:1	9.30±0.3 × 10^6
AgNSB	Jo et al., 2014	1:1	5.93 ±1.0 × 10^6
NAP	Lupaescu et al., 2019	1:1	8.14 ±0.7 × 10^5
IH6	Guo et al., 2019	1:1	7.68 ±1.0 × 10^5
Peptide VIII	–	1:1	2.13 ±0.4 × 10^7
Peptide IX	–	1:1	2.07 ±0.8 × 10^6
Peptide X	–	1:1	5.09 ±0.6 × 10^5
Peptide XI	–	1:1	3.70 ±0.5 × 10^5
A1	–	1:2	1.12 ±0.5 × 10^6
A2	–	1:2	2.22 ±0.8 × 10^6

"-" indicates the peptides or ssDNA of de novo design.

$$K_a^{AgT_n} \Big/ K_a^{AgP} = \frac{[AgT_n]}{[Ag]\cdot[T]^n} \cdot \frac{[Ag]\cdot[P]}{[AgP]}$$
$$= \left([P]_0 - [Ag]_0 + [\alpha]\right)\cdot\left[\alpha\right] \Big/ \left\{\left([Ag]_0 - [\alpha]\right)\cdot\left([T]_0 - n\cdot[\alpha]\right)^n\right\}$$

The $KAgT_n$ a value means the stability constant of the AgT_n complex, thus indicating the affinity of Ag(I) to the target.

3. Results and discussion

3.1. Design of the peptide ligand

Selecting a suitable ligand of well-defined Ag(I) binding affinity is the top priority. We leveraged previous works in conducting the investigation. In view of the designability and biocompatibility of peptides, our group has put forward an original peptide RFPRGGDD that is capable of recognizing Ag(I) selectively [7]. The most striking observation to emerge from the study is the ability of Ag(I) to induce conformational transitions from the unfolded to the folded state through interaction with the side chains of appropriately placed amino acid ligands within the peptide. It has also been proven that the peptides containing RRDD sequence possess the combination ability with Ag(I). This behavior basically benefited from the 4-coordination of Ag(I) with the carboxyl oxygen and amino nitrogen [7]. In this context, six kinds of peptides containing Arginine (R) and Aspartic acid (D) were devised to support an Ag(I) binding motif. Particularly, the amino acids R and D are respectively arranged at opposite ends of the peptide, conducing to the conformational transition during the process of Ag(I) composite formation. To some extent, additions and deletions of inner amino acids contribute to the shape of the typical peak. As shown in Fig. 1A, the best performance came from the peptide RFPRDD, whose structure and stability was respectively demonstrated in Fig. 1B and Figure S1. The setting of R and D at the terminal served to generate the 4-coordinated complexes with Ag(I). It was evident that the synergistic effect of Phenylalanine (F) and Proline (P) could produce a more characteristic peak. Notably, there appeared to be positional conservation that the identified positions of F and P were not supposed to vary. For the sake of clarity RFPRDD will be written P and the Ag(I)-RFPRDD will be noted AgP.

The conformation of the peptide RFPRDD was characterized in pH 7.4 PB by circular dichroism (CD). There was significant difference in the mean residue ellipticity after introducing Ag(I) into the system, consistent with the change of secondary structure in the integrating process (Fig. 2A). We concluded from the evidence that Ag(I) could effectively drive the conformation transition of a de novo designed peptide, consequently resulting in a specific complexing form. To strengthen the action, the effects of the pH and the PB concentration were carefully discussed. In the case, the PB concentration shows strong influence on the absorbance measurements. This is mainly because the conformation of peptides could be affected by the buffer concentration, owing to the change of electrostatic effect (Figure S2) [34,35]. The results revealed that 10 mM of PB at pH 7.4 was the necessary condition to reach the optimal performance, which was judged according to its distinct advantages in peak shape. Fig. 2B demonstrated the typical series of spectra obtained from AgP complexes. With the increase of Ag(I) concentrations in a certain range, the more specific absorption could be observed until the saturation of combination, the linear response of which was shown in Figure S3. Then, MALDI-TOF Mass spectrometer was employed to describe the coordination mode of RFPRDD and Ag(I) at different dosages. The coordination ratio 1:1 occurred where a small or moderate quantity of Ag(I) is involved because of the existence of m/z = 913 (Fig. 2C and D). Once Ag(I) became excessive, there would be multiple coordination forms of RFPRDD and Ag(I) at 1:1, 1:2, 1:3, 1:4 and 1:5 (Fig. 2E). To simplify and unify the way in which subsequent calculation was conducted, the ratio 1:1 was identified as the coordination behavior by appropriately controlling the Ag(I) concentrations.

Then, the formation time of AgP complexes was investigated by kinetics measurements. Fig. 2F gave a view of the representative kinetic curves of the absorbance at 300 nm with incubation time. The entire combination could be fulfilled in 80 s, regardless of Ag(I) concentrations. And high selectivity of RFPRDD to Ag(I) was also displayed in Figure S4. Therefore, the binding process of RFPRDD and Ag(I) was superior over other coordination methods in rapid complexing [7–10]. This trend reflects the high efficiency and simplicity of our procedure, avoiding the problems of long-time incubation and multi-step operation in other strategies.

3.2. Quantification of Ag(I) binding affinity to RFPRDD

It is certain that, the essential parameter of the peptide RFPRDD is its affinity constant for Ag(I). This assessment was implemented via the competition of EDTA, who held definite affinity and coordination ratio with Ag(I) [29]. The competition experiments were constituted by the chelation of EDTA to remove silver ions from the colored AgP complexes, causing a reduction of the characteristic signature and the color fading (Figure S5A). These typical absorption peaks were indicative of the existence of AgP complexes in the system (Fig. 3A). The RFPRDD was first added (dotted line), then Ag(I) (black solid line), and then successive additions of the EDTA were performed (colored lines). Blank AgP complexes had a maximum absorption at λ_{max} = 300 nm. The introduction of EDTA gave rise to a decrease of absorbance values. This is primarily because of the disintegration of AgP complex under the circumstances of EDTA competition. In Figure S5B, the determined 1:1 (EDTA: Ag(I)) molar ratio was confirmed by the employment of MALDI-TOF Mass, consistent with the published information [29]. Through the calculation where the inferential reasoning and analysis had been described in detail, the affinity value of $K^{AgP}{}_a = 8.19 \pm 0.4 \times 10^7\ M^{-1}$ was obtained and used for further study. And the computational

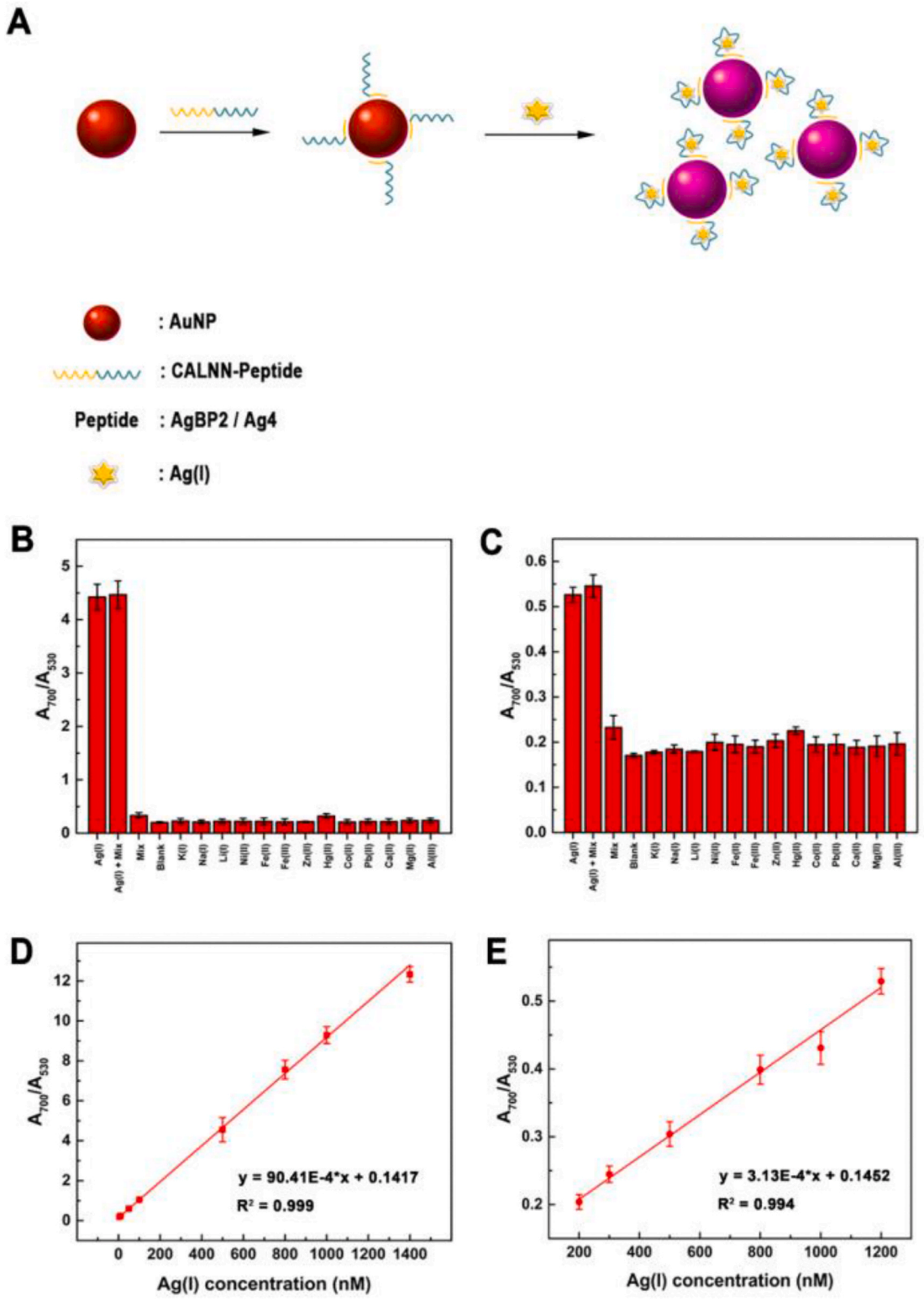

Fig. 4. (A) Schematic illustration for the Ag(I) detection using different sensing elements. The selectivity of (B) the AgBP2-mediated assay or (C) the Ag4-mediated assay for Ag(I). In the measurement, the concentration of other metal ions was 100-fold higher than that of Ag(I). (D) The response linearity of the AgBP2-mediated assay at the Ag(I) concentration range of 5–1400 nM. (E) The response linearity of the Ag4-mediated assay at the Ag(I) concentration range of 200–1200 nM.

proceeding was clearly stated in the theoretical calculations of Supporting Information.

After taking this affinity value, the peptide was selected to construct a competition experiment as a suitable Ag(I) ligand. In Scheme 1, the peptide ligand reacted with Ag(I) to yield the 1:1 complexes (AgP) who had clear formation constants. When the target was added, there would be a competition for Ag(I). Meanwhile, variations could be apparent in the characteristic signals of AgP complexes. And shifts of this coordination equilibrium also brought with visible changes in color of the solution.

3.3. Reliability of the quantification

As a newly proposed strategy, it is demanded to have a high veracity of measurement. To show the reliability, the affinities were calibrated with three amino acids (Histidine, Methionine and Tryptophan) as the well-documented affinity standards. We respectively discussed their coordination numbers with Ag(I) by using the MALDI-TOF Mass. Figure S6 revealed all of them had the same proportions in binding experiments, two equivalents of who were bound with one equivalent of Ag(I). Additionally, the corresponding behavior was displayed in Figure S7. The absorbance at $\lambda = 300$ nm of the mixture was plotted as a function of equivalent numbers of the amino acid added (Fig. 3B). Then, these data were entered into the calculation procedure, which was explicitly depicted in the theoretical calculations of Supporting Information. The affinity values obtained in the proposed platform are gathered in Table S3. Qualitative analysis indicated that the Ag(I) affinities of three amino acids were in conformity to the results from previous researches [30–32]. This trend gave a reasonable explanation that our project were equipped with great reliability and feasibility.

3.4. Biomolecules affinities for Ag(I)

The great potential of the approach in application was illustrated by testing the relevant biomolecules interacting with Ag(I). Silver binding peptides (e.g. AgBP2, Ag4, AgP35, AgNSB, IH6, NAP, NAPC) have been identified by phage display technology or a series of practical experiments. These peptides are widely utilized to take part in the silver material synthesis or biosensing, owing largely to their specific affinity to silver ions and the conformational transition during the combination. The current dilemma lies in the insufficient researches on estimating their affinity values, although it is highly required to supply direct and quantifiable data to compare the affinity abilities. In response to this situation, the proposed strategy was used for computing the Ag(I) affinities of silver binding peptides, as well as a series of artificially designed peptides and the related ssDNA. The coordination modes of Ag(I) to detection targets were explored first as depicted in Figure S8–S11. The results indicated that the given peptides had the equivalent performance in binding to Ag(I) at 1:1 while the ssDNA to Ag(I) at 1:2. Considering the distinctive combination ratio of ssDNA: Ag(I), the corresponding composition principle was further interpreted in Figure S12. Through establishment of the coordination competition, absorbance values could be monitored and their fits are shown in Figure 3C, D and S13. In accordance with the individual behaviors in combination, the specific molar absorption coefficient (ε) and coordination ratio (n) were identified and put into the calculating equation, which was fully demonstrated in the theoretical calculations (Supporting Information). All the Ag(I) affinity values obtained in the present study are gathered in Table 1. The successful application in different varieties of targets implied the excellent universality and potential of our project.

3.5. Application and potential for biosensing

Selecting a proper sensitive element occupies an indispensable position in building a testing platform. Pursuing a convenient method for characterization, evaluation and optimization of this capture unit, therefore, becomes the hot research task. With the current protocol, the goals could be achieved by accurately assessing the affinity values of biomolecules. To ensure the fundamental role of strategy in biosensing, peptides AgBP2 and Ag4 were employed respectively as sensitive parts, who had the definitive Ag(I) affinity constants derived here. As shown in Fig. 4A, a detecting device was established on the foundation of specific binding of these two peptides to Ag(I). The entire process was divided into two steps that were the modification step and the reaction step. First, the given peptides were stably decorated on AuNPs by the anchor CALNN [33–36]. Then, the aggregation of peptide-AuNPs was stimulated by adding the target Ag(I), hence triggering distinct colorimetric responses (A_{700}/A_{530}). The behavior owed much to the reduce of electrostatic repulsion and steric hindrance between nanoparticles [7].

In this case, we estimated several parameters, namely, the PB concentration, the pH of solution, the AuNPs diameter, and the reaction time. To boost the sensitivity of the detaction, 10 mM PB at pH 7.4 and 30 nm-sized AuNPs were chosen. The reaction times of AgBP2 and Ag4 were respectively 10 min and 20 min (Figure S14). For the purpose of conducting a contrastive study, the selectivity and the linear curves of two systems were given in Fig. 4. By means of the exhaustive analysis, the estimated limits of detection for each peptide were 2 nM (AgBP2), 75 nM (Ag4). Taken the shorter reacting time, lower determination limit and wider linear area of AgBP2-mediated sensing into account, the AgBP2 exhibited higher capability to capture Ag(I), fully in conformity with the conclusion from our results computed. The validity and availability of our project was corroborated in sensing selection among multiple elements. As a consequence, the direct and precise determination of Ag(I) affinity informed reasonable expectations in choosing the suitable capture molecules and further planning the biosensor.

4. Conclusion

In summary, a new peptide ligand RFPRDD for Ag(I) was engineered and their complexes with typical ultraviolet absorption at $\lambda = 300$ nm were comprehensively characterized. It was engaged in straightforwardly determining the affinity constants of Ag(I) for biomolecules by UV–vis competition experiments. The obtained affinities of three amino acids (Histidine, Methionine and Tryptophan), agreed perfectly with that of published researches. We take this as evidence that the strategy was equipped with the high dependability and accuracy. The practical applicability was also validated by measuring the Ag(I) affinities of a variety of peptides and ssDNA, like Ag-binding peptides involving AgBP2, Ag4, AgP35. More, the biosensors were arranged to highlight the key role of the strategy that could provide easy access to direct acquisition and comparison of Ag(I) combining capacity of recognition elements. As a calculated reference standard, this determination had the potential to be of great benefit to the design and optimization of sensing components, thus facilitating the construction of sensors. Based on the principle of calculation, we also hypothesize that there is great probability to generalize the approach to appraise affinities of any other metal ions to various biomolecules.

Declaration of competing interest

The authors declare that they have no known competing financial interests or personal relationships that could have appeared to influence the work reported in this paper.

Acknowledgment

This work was financially supported by The National Natural Science Foundation of China (NSFC) (Nos. 21775114, 21874102).

Appendix B. Supplementary data

Supplementary data to this article can be found online at https://doi.org/10.1016/j.talanta.2021.122089.

References

[1] S. Chernousova, M. Epple, Silver as antibacterial agent: ion, nanoparticle, and metal, Angew. Chem. Int. Ed. 52 (2013) 1636–1653.
[2] B. Le Ouay, F. Stellacci, Antibacterial activity of silver nanoparticles: a surface science insight, Nano Today 10 (2015) 339.
[3] K.Y. Zheng, M.I. Setyawati, D.T. Leong, J.P. Xie, Antimicrobial silver nanomaterials, Coord. Chem. Rev. 357 (2018) 1–17.
[4] T. Li, L.L. Shi, E.K. Wang, S. Dong, Silver-ion-mediated DNAzyme switch for the ultrasensitive and selective colorimetric detection of aqueous Ag^{+} and cysteine, Chem. Eur J. 15 (2009) 3347–3350.

[5] R.F. Zou, Q. Wang, J.C. Wu, J.X. Wu, C. Schmuck, H. Tian, Peptide self-assembly triggered by metal ions, Chem. Soc. Rev. 44 (2015) 5200–5219.
[6] M. Reithofer, R.A. Lakshmanan, A.T. Ping, J.M. Chin, C.A.E. Hauser, In situ synthesis of size-controlled, stable silver nanoparticles within ultrashort peptide hydrogels and their anti-bacterial properties, Biomaterials 35 (2014) 7535–7542.
[7] X. Li, Z. Wu, X. Zhou, J. Hu, Colorimetric response of peptide modified gold nanoparticles: an original assay for ultrasensitive silver detection, Biosens. Bioelectron. 92 (2017) 496–501.
[8] S. Ghosh, S. Verma, Metalated peptide fibers derived from a natural metal-binding peptide motif, Tetrahedron Lett. 48 (2007) 2189–2192.
[9] S.N. Dublin, V.P. Conticello, Design of a selective metal ion switch for self-assembly of peptide-based fibrils, J. Am. Chem. Soc. 130 (2008) 49–51.
[10] T. Sawada, A. Matsumoto, M. Fujita, Coordination-driven folding and assembly of a short peptide into a protein-like two-nanometer-sized channel, Angew. Chem. Int. Ed. 53 (2014) 7228–7232.
[11] R.R. Naik, S.E. Jones, C.J. Murray, J.C. McAuliffe, R.A. Vaia, M.O. Stone, Peptide templates for nanoparticle synthesis derived from polymerase chain reaction-driven phage display, Adv. Funct. Mater. 14 (2004) 25–30.
[12] R.R. Naik, S.J. Stringer, G. Agarwal, S.E. Jones, M.O. Stone, Biomimetic synthesis and patterning of silver nanoparticles, Nat. Mater. 1 (2002) 169–172.
[13] M.B. Dickerson, K.H. Sandhage, R.R. Naik, Protein- and peptide-directed syntheses of inorganic materials, Chem. Rev. 108 (2008) 4935–4978.
[14] E. Lee, D.H. Kim, Y. Woo, H.G. Hur, Y. Lim, Solution structure of peptide AG4 used to form silver nanoparticles, Biochem. Biophys. Res. Commun. 376 (2008) 595–598.
[15] X. Zhang, P. Yang, W. Yang, J. Chen, The bio-inspired approach to controllable biomimetic synthesis of silver nanoparticles in organic matrix of chitosan and silver-binding peptide (NPSSLFRYLPSD), Mater. Sci. Eng. C 28 (2008) 237–242.
[16] A.C. Heather, D. Olivier, R.N. Rajesh, C.P. Carole, L.K. David, Genetically engineered chimeric silk–silver binding proteins, Adv. Funct. Mater. 21 (2011) 2889–2895.
[17] Y.K. Jo, J.H. Seo, B.H. Choi, B.J. Kim, H.H. Shin, B.H. Hwang, H.J. Cha, Surface-independent antibacterial coating using silver nanoparticle-generating engineered mussel glue, ACS Appl. Mater. Interfaces 6 (2014) 20242–20253.
[18] R.H. Sedlak, M. Hnilova, C. Grosh, H. Fong, F. Baneyx, D. Schwartz, M. Sarikaya, C. Tamerler, B. Traxler, Engineered escherichia coli silver-binding periplasmic protein that promotes silver tolerance, Appl. Environ. Microbiol. 78 (2012) 2289–2296.
[19] Y. Guo, S. Wang, H. Du, X. Chen, H. Fei, Silver ion-histidine interplay switches peptide hydrogel from antiparallel to parallel β-assembly and enables controlled antibacterial activity, Biomacromolecules 20 (2019) 558–565.
[20] A.V. Lupaescu, M. Jureschi, C. Ciobanu, I.L. Ion, G. Zbancioc, B.A. Petre, G. Drochioiu, FTIR and MS evidence for heavy metal binding to anti-amyloidal NAP-Like peptides, Int. J. Pept. Res. Therapeut. 25 (2019) 303–309.
[21] S. Brown, M. Sarikaya, E.J. Johnson, A genetic analysis of crystal growth, Mol. Biol. 299 (2000) 725–735.
[22] J.N. Cha, G.D. Stucky, D.E. Morse, T.J. Deming, Biomimetic synthesis of ordered silica structures mediated by block copolypeptides, Nature 403 (2000) 289–292.
[23] T. Douglas, E. Strable, D. Willits, A. Aitouchen, M. Libera, M. Young, Protein engineering of a viral cage for constrained nanomaterials synthesis, Adv. Mater. 14 (2002) 415–418.
[24] A.C. Daban, V. Borghesani, S. Sayen, E. Guillon, Y. Journaux, G. Gontard, L. Lisnard, C. Hureau, Link between affinity and Cu(II) binding sites to amyloid-β peptides evaluated by a new water-soluble UV-visible ratiometric dye with a moderate Cu(II) affinity, Anal. Chem. 89 (2017) 2155–2162.
[25] I. Zawisza, M. Rozga, W. Bal, Affinity of copper and zinc ions to proteins and peptides related to neurodegenerative conditions (Aβ, APP, α-synuclein, PrP), Coord. Chem. Rev. 256 (2012) 2297–2307.
[26] B. Alies, E. Renaglia, M. Rozga, W. Bal, P. Faller, C. Hureau, Cu(II) Affinity for the alzheimer's peptide: tyrosine fluorescence studies revisited, Anal. Chem. 85 (2013) 1501–1508.
[27] T.R. Young, A. Kirchner, A.G. Wedd, Z. Xiao, An integrated study of the affinities of the Aβ16 peptide for Cu(I) and Cu(II): implications for the catalytic production of reactive oxygen species, Metallomics 6 (2014) 505–517.
[28] G. Arena, G. Papppalardo, I. Sovago, E. Rizzarelli, Copper(II) interaction with amyloid-β: affinity and speciation, Coord. Chem. Rev. 256 (2012) 3–12.
[29] G.L. Miessler, D.A. Tarr, Inorganic Chemistry, fourth ed., Prentice Hall, New Jersey, 2010.
[30] Y.H. You, C.P. Zhang, Interaction between silver ions and histidine, J. Clin. Rehabilitative Tissue Eng. Res. 14 (2010) 5498–5504.
[31] B.K. Wang, Experiment on Medium Inorganic Chemistry, Nanjing University Press, Nanjing, 1998.
[32] Y. You, Study on the Mechanism of Reaction between Amino Acid and Silver Ion and Preparation of Amino Acid-Silver Nanoparticles, Guizhou University Press, Guizhou, 2006.
[33] X.Y. Li, F.F. Feng, X.D. Zhou, J.M. Hu, Rational design of an anchoring peptide for high-efficiency and quantitative modification of peptides and DNA strands on gold nanoparticles, Nanoscale 10 (2018) 11491–11497.
[34] Z. Wu, Y. Liu, Y. Liu, H.M. Xiao, A.G. Shen, X.D. Zhou, J.M. Hu, A simple and universal "turn-on" detection platform for proteases based on surface enhanced Raman scattering (SERS), Biosens. Bioelectron. 65 (2015) 375–381.
[35] Z. Wu, Y. Liu, X.D. Zhou, A.G. Shen, J.M. Hu, A "Turn-Off" SERS-based detection platform for ultrasensitive detection of thrombin based on enzymatic assays, Biosens. Bioelectron. 44 (2013) 10–15.
[36] R. Levy, N.T.K. Thanh, R.C. Doty, I. Hussain, R.J. Nichols, D.J. Schiffrin, M. Brust, D.G. Fernig, Rational and combinatorial design of peptide capping ligands for gold nanoparticles, J. Am. Chem. Soc. 126 (2004) 10076–10084.

Xin-Yi Li received the PhD degree in Wuhan University. Her current research interests are the behavior between peptides and metal ions. She mainly focuses on the design of peptides and explore their application in biomolecule detection.

Xiao-Dong Zhou is a professor at Wuhan University, PR China. His research field is the preparation of metal-organic complexes and their analysis applications.

Ji-Ming Hu received the PhD degree in Wuhan University. Currently he is a professor at the College of Chemistry and Molecular Sciences, Wuhan University. He focuses on Raman spectra study and their application based on the Surface Enhanced Raman Scattering.